Comptes rendus - Geoscience 351 (2019) 375–383

Contents lists available at ScienceDirect

Comptes rendus - Geoscience

www.journals.elsevier.com/comptes-rendus-geoscience

Hydrology, Environment (Geomorphology)

Morphometric analysis of the drainage network of Samos Island (northern Aegean Sea): Insights into tectonic control and flood hazards

Nikos Charizopoulos [a, *], Panagiotis Mourtzios [b], Thomas Psilovikos [c], Aris Psilovikos [b], Lina Karamoutsou [b]

[a] Agricultural University of Athens, Laboratory of Mineralogy–Geology, Iera Odos 75, 118 55 Athens, Greece
[b] University of Thessaly, Department of Ichthyology and Aquatic Environment, Odos Fitokou, 384 46 Volos, Greece
[c] Aristotle University of Thessaloniki, Department of Forestry and Natural Environment, Laboratory of Engineering Sciences and Topography, 54124, Thessaloniki, Greece

ARTICLE INFO

Article history:
Received 5 September 2018
Received in revised form 14 February 2019
Accepted 12 March 2019
Available online 25 May 2019
Handled by Isabelle Manighetti

Keywords:
Morphometric analysis
Hydrographic network
Tectonic control
Samos island

ABSTRACT

The morphometric analysis of alluvial drainage provides insights into its dynamics, erosion capacity, susceptibility to floods and possible genetic relations to tectonic faulting. In this study, we analysed the drainage system of Samos Island, located in the northern Aegean Sea. The results indicate a vulnerability to erosion and flooding events, and these intense phenomena concentrate mostly on third-order catchments. Two dissimilar drainage network systems are shown: an older drainage network system with a main NW–SE direction, which includes fourth- and fifth-order branches, and a recent drainage network system, which includes new, smaller order branches with a main NE–SW direction. The major tectonic fault orientations are NNW–SSE. The branches of the hydrographic network and faults present different directions, which indicates that the hydrographic pattern is not affected by tectonics.

1. Introduction

Morphometry is the measurement and mathematical analysis of the configuration, shape, and dimension of the Earth surface and its landforms (Hajam et al., 2013; Pareta and Pareta, 2011). The morphometric analysis of alluvial drainage provides insights on its dynamics, erosion capacity, susceptibility to floods, etc., as on its possible genetic relations to tectonic faulting. The principal morphometric parameters that are commonly analyzed include the hierarchical order of the various streams – from principal (order-1) to smaller (order-*n*) bifurcating streams – of the whole basin area and slopes, the length of the drainage channels, their density (*D*) – the aggregate length of streams per unit area – and frequency (*F*) – the numbers of streams per unit area –, and the bifurcation ratio (*Rb*) (Kumar et al., 2000; Verstappen, 1983). Pioneering works on drainage basin morphometry were performed by Horton (1932) and Strahler (1952). Building on these landmark works, more recent studies were conducted using the benefit of GIS representations. Altogether, these studies show that drainage morphology and hence morphometry are intimately controlled by erosional processes (Dash et al., 2014; Kumar et al., 2018; Ngapna et al., 2018), flooding events (Arnous and Omar, 2018; Bhagwat et al., 2011; Jahan et al., 2018) and tectonics (Argyriou et al., 2017; Bahrami, 2013; Ntokos, 2017; Ribolini and Spagnolo, 2008).

Here we analyze the drainage system of Samos Island, one of the largest Islands of Greece. The Island presents a

* Corresponding author.
E-mail address: nchariz@gmail.com (N. Charizopoulos).

https://doi.org/10.1016/j.crte.2019.03.001
1631-0713/

vulnerability to erosion and flooding events and has been affected many times in the past by such natural hazards (Kotinas, 2014). In such areas where flash floods are frequent, a morphometric analysis is one of the most important tools to determine and evaluate the responses of the drainage basin to drainage characteristics and flash flood hazard (Angilliri, 2008; Perucca and Angilieri, 2010). Moreover, morphometric parameters for stream networks, drainage basins, and relief can be used to investigate the erosion status and the interplay between the tectonic processes and the morphology of the drainage basin (Argyriou et al., 2017). In this research, the catchment length, area, and slopes were measured using available topographic maps and GIS software and the stream hierarchical ranks were defined according to Strahler's classification (Strahler, 1952). The bifurcation ratio, stream total number and length, drainage density, and channel frequency were determined according to Horton's laws (Horton, 1932, 1940, 1945). The relief ratio and the hypsometric integral were calculated using standard methods (Keller and Pinter, 2002; Schumm, 1956). The effects of tectonics on the drainage network were examined by comparing the orientations of the known tectonic faults and the directions of the branches of the drainage network (use of rose diagrams/plots).

From this analysis, we discuss (a) the erosional processes and flood events in the third-, fourth-, and fifth-order catchments of Samos Island and (b) the controls of the tectonic faults on the development of the drainage network of Samos Island.

2. Site description, materials, and methods

2.1. Site description

The Island of Samos is situated at the eastern end of the central Aegean Sea and is 1.2 km away from the Turkish coastline. Samos has a coastline length of 160.9 km, a major axis of 43 km, a minor axis of 19 km and a surface area around 480 km^2 (Fig. 1a). The mean yearly precipitation and temperature in Samos for the period 1950–2007 are 790 mm and 17.9 °C, respectively (http://www.hnms.gr/emy/el/). Following the Köppen–Geiger climatic characterization (Peel et al., 2007), Samos Island is under a Mediterranean Climate, in Csa class. The precipitation gets its highest values from November to February, with a normal month height of more than 100 mm. This commonly induces extreme flooding events. Precipitations are almost null from June to August. In the remaining of the year, the precipitations range between 25 and 90 mm.

2.1.1. Geomorphology

Samos Island is divided into five geomorphological units related to the presence of individual massifs: (a) the eastern Samos karst range, (b) the Neogenic deposits in eastern Samos, (c) central Samos, (d) the Neogenic deposits in western Samos and (e) western Samos. The hill “Zoodochos Pigi” (433 m), the “Ampelos” (1150 m), and the “Kerketeas” (1433 m) mountains occupy the eastern, central, and western parts of Samos, respectively. Among them are two Neogenic basins, the “Karlovasion” and the “Mytilinii”" (Fig. 1b). The mountainous northwestern part of the island presents steep cliffs, while the coastal topography gradient is high and coasts are mostly fault-controlled (Vassilopoulos et al., 2008). The high and steep relief, the rough topography of the close-by Turkish coastline and the geographic position of Samos Island in the northern Aegean make it prone to extreme winter precipitation events (Psilovikos Ar et al., 2003, 2004). The vegetation of Samos is dense; many springs outflowing even in summer and small streams of torrential type exist also on the Island (Mourtzios et al., 2009).

2.1.2. Geology

Samos Island belongs to the Attic–Cycladic Blueschist Unit (Vassilopoulos et al., 2008). A characteristic feature of the formations of this unit is that they have been metamorphosed at high-pressure and low-temperature conditions, resulting in the frequent occurrence of blue schists. On Samos Island, two main Neogene basins were developed. The Mytilinii basin, situated in eastern Samos, and the Karlovassi basin, situated in the west (Kantiranis et al., 2004). The pre-Neogene basement of both basins comprises four tectonic units containing marbles, dolomites, quartzites, phyllites, metamorphic basic to ultrabasic rocks, and a more youthful nappe of diabases, peridotites, cherts, and limestones (Stamatakis, 1989a, 1989b). The deposits of both basins are upper Miocene to Pliocene in age and are probably a mainland facies (Dermitzakis and Papanikolaou, 1981). At the margin of the basin, there are events of rhyolites, dacites, trachytes, and basalts of Neogene age (Kantiranis et al., 2004).

2.2. Materials

We used two topographic maps from the Hellenic Military Geographical Service namely the sheets “Samos” and “Neon Karlovasion” (HMGS, 1978) and two geological maps of the Institute of Geology and Mineral Exploration, namely the sheets “Samos” and “Neon Karlovasion” (IGME, 1985), in 1:50,000 scale. The meteorological data were taken from the Hellenic National Meteorological Service for the Samos Airport hydrometeorological station, which is in the southern part of the island (http://www.hnms.gr/emy/el/). Finally, ArcGIS 9.3 Software by ESRI was used for the production of the digital geodatabase.

2.3. Methodology

Using the ArcGIS 9.3 software and the maps specified above, we conducted the following steps: (i) digitizing of the large-scale, overall hydrographic network of Samos Island; (ii) digitizing of the third-, fourth-, and fifth-order catchments in the Samos basins; (iii) establishing the hierarchy and numbering of the hydrographic network, following Strahler (1952); (iv) recovering the topography of the zone by digitizing the contour lines every 20 m as the trigonometrical points. From this information, we created a Digital Elevation Model (DEM), with a pixel size of 20 m (both horizontal and vertical). (v) We also digitized the coastline, the geologic formations, and all the tectonic faults shown on the available maps. Then, we referenced all

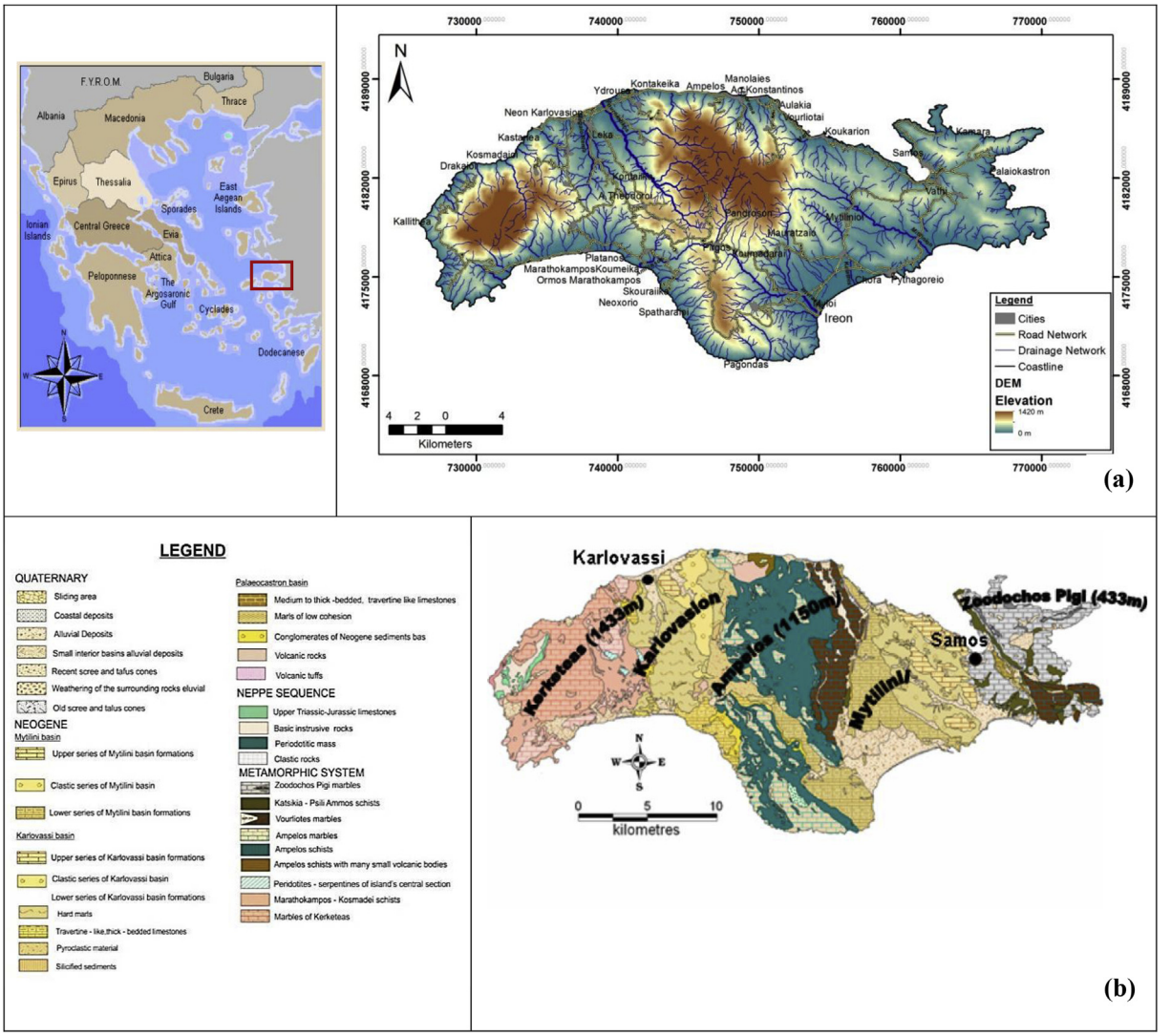

Fig. 1. (a) Samos Island in the Hellenic Territory. (b) Geological map of Samos Island.

the data in GIS software and measured the catchment's length and area and stream hierarchy following Horton's first and second laws (Horton, 1932, 1940, 1945). We also measured the number of streams, the length and mean length for each hierarchical order, the total number of streams and their lengths, the bifurcation ratio and mean bifurcation ratio, the theoretically expected number for the number of streams and mean length of streams (indicated as ideal values), and the drainage density and channel frequency based on Horton's laws. The minimum, maximum, and mean altitudes of the catchment were computed providing inputs for the calculation of relief ratio and hypsometric integral (Table 1) according to Schumm (1956) and Keller and Pinter (2002) methods respectively and a slope map from the DEM (in degrees) was measured. The Geodetic Reference System is the Hellenic Geodetic Reference System 1987 (EGSA ′87). Finally, using Georient v.9.2 software rose diagrams – plots (*Rf*) of the stream directions per order and for the tectonic faults, orientations for each one of the five geomorphological units of Samos Island were constructed.

3. Results and discussion

3.1. Digitizing and numbering of the hydrographic network

The branches of the entire hydrographic network were numbered according to Strahler (1952) (Fig. 2) and we focused on the third-, fourth-, and fifth-order catchments (Fig. 3a–c). Their pattern is dendritic, and the aggregate number of streams (ΣNu) is 1162, while their aggregate length (ΣLu) is 834.15 km (Table 2). The aggregate number of the catchments is 47, 10, and 2 for the third-, fourth-, and fifth-orders, respectively (Fig. 3a–c). The main drainage

Table 1
Morphometric parameters of the catchment area of Samos Island.

Parameter	Formula	Description	References
Horton's first law of stream numbers	$Nu = \overline{Rb}^{K-u}$	The numbers of streams of successively lower orders in a given catchment tend to form a geometric progress	Horton (1940)
Horton's second law of stream lengths	$\sum \overline{Lu} = \overline{L_1}\,\overline{RL}^{u-1}$	The mean stream length segments of each of the successive orders tend to approximate a direct geometric series with stream length increasing towards a higher order of streams	Horton (1940)
Drainage density, D (km^{-1})	$D = \frac{\sum L}{A}$	The aggregate length of streams per unit area	Horton (1945, 1932)
Channel frequency, F (km^{-2})	$F = \frac{\sum Nu}{A}$	The total number of streams per unit area	Horton (1945, 1932)
Relief ratio, Rh (%)	$Rh = \frac{H}{Lbu_{max}}$	The ratio of basin relief to basin length	Schumm (1956)
Hypsometric integral, H_I (%)	$H_I = \frac{H_m - H_{min}}{H_{max} - H_{min}}$	The area below the hypsometric curve, which represents the relative proportion of the watershed area below (or above) a given height	Keller and Pinter (2002)

where Nu = ideal value for the number of streams of order u, $\overline{Rb}$ = mean bifurcation ratio ($Rb = \frac{Nu}{Nu+1}$ (Nu: the number of streams of order u)), K = maximum order of the streams, u = streams of a given order, $\Sigma\overline{Lu}$ = ideal value for the channel mean length of order u, $\overline{L_1}$ = mean channel length of first order, $\overline{RL}$= mean length ratio ($RL = \frac{\overline{Lu}}{\overline{Lu}-1}$ ($\overline{Lu}$: mean channel length of order u)), ΣL = total channels length (km), A = catchment area (km^2), ΣNu = total number of streams, $H = H_{max} - H_{min}$ (m), Lbu_{max} = maximum length of the catchment (km) (Apollov, 1963), H_m = mean altitude of the catchment (m), H_{min} = minimum altitude of the catchment (m), H_{max} = maximum altitude of the catchment (m)

divide (Fig. 2 – red line) in the center separates the island into northern and southern catchments. In the Neogenic deposits in eastern Samos, the catchments on the northern side are significantly smaller than the catchments on the southern side. The inverse occurs in the Neogenic deposits in the western part of Samos. The catchments in the southern part are smaller than the northern ones and moreover, the hydrographic network is more developed in this area. In the east, small branches of streams are found because of karstic phenomena (Cooper et al., 2011) (Fig. 2 – light blue circle).

3.2. Horton's first law

The analysis of the number of streams in the study area is presented in Table 2. As shown, the higher the order, the lower the number of streams. This means that all order catchments follow Horton's first law. The bifurcation ratio ranges from 3.71 to 5. These values are typically found in zones where geologic structures do not exert any significant impact on the drainage pattern (Waikar and Nilawar, 2014). Within the range of 3–5, higher Rb values can be indicative of structural complexity and low permeability

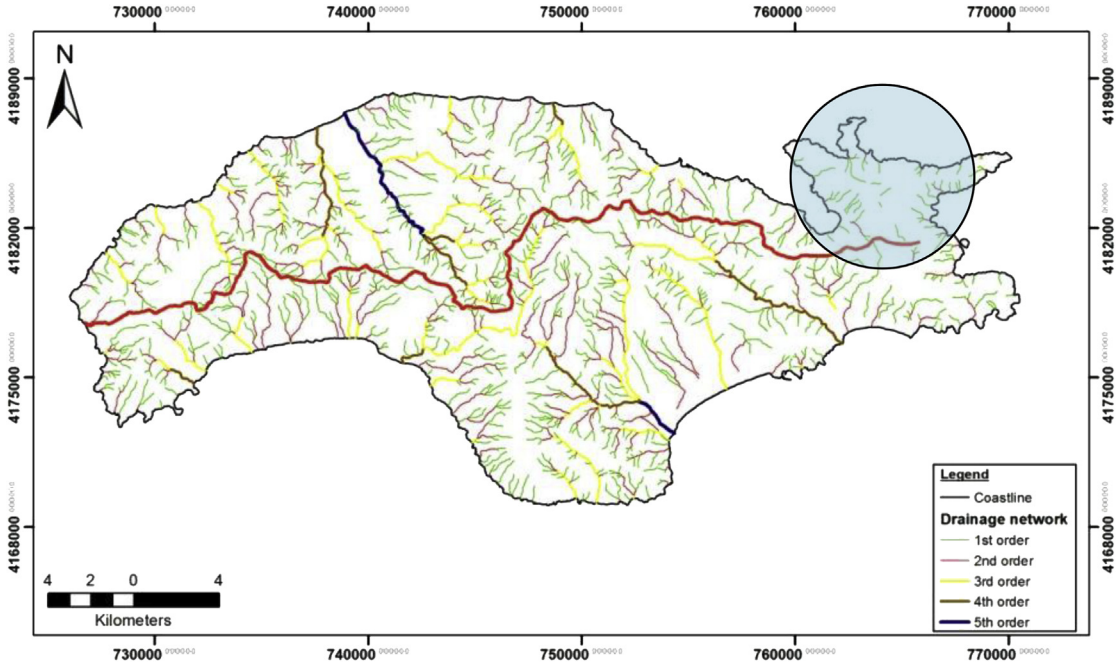

Fig. 2. The hydrographic network stream order of Samos Island according to Strahler (1952) with the main drainage divide (red line).

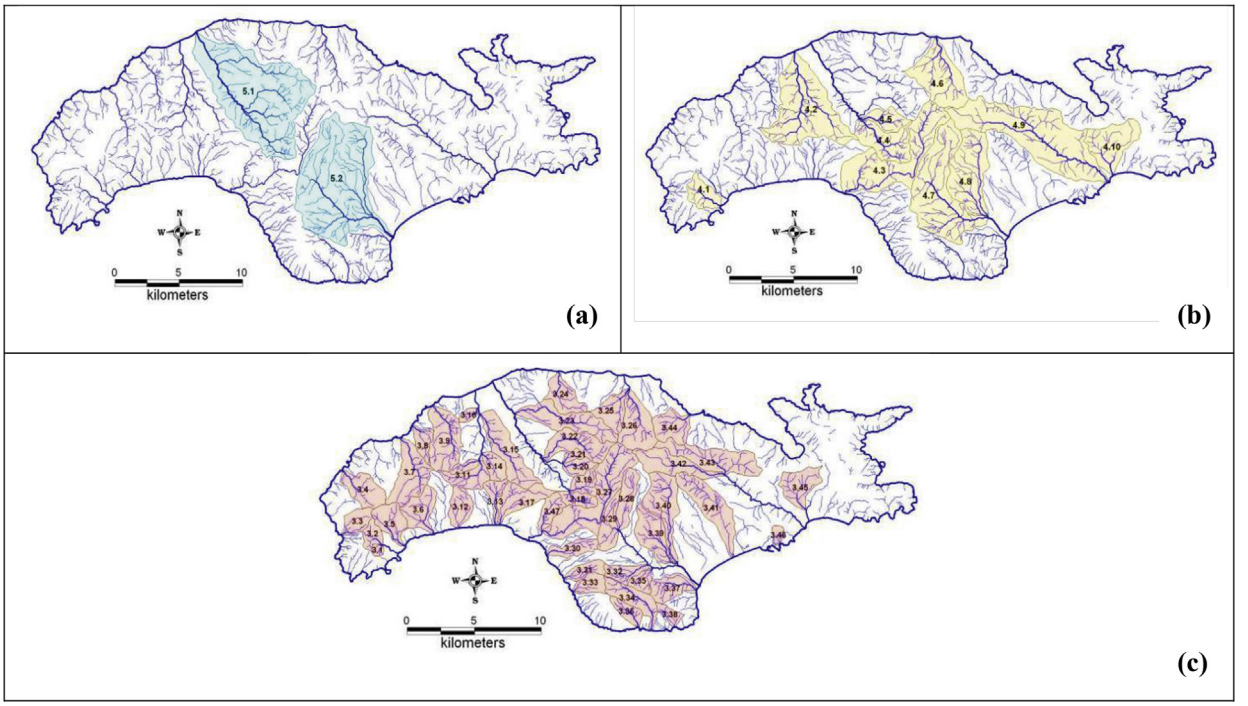

Fig. 3. Thematic maps of Samos Island hydrographic network order catchments according to Strahler (1952): (a) third-order catchments, (b) fourth-order catchments, (c) fifth-order catchments.

(Argyriou et al., 2017). The mean bifurcation ratio ($\overline{Rb}$) is 4.60 (Table 2). As indicated by Shreve (1966), the "theoretical" ($\overline{Rb}$) value is 4.00 and is found in areas where the geologic structures do not distort the drainage pattern (Strahler, 1964). The numbers of hydrographic network stream orders are larger than the theoretically expected values presenting a critical positive deviation from 93.97 to 141.23% for all orders, with major differences in the second (141.23%) and the third (123.80%) orders (Table 2, Fig. 4a).

3.3. Horton's second law

The analysis of the lengths of the streams in the study area is shown in Table 2. It is observed that the average stream length increases towards a higher order of streams for all order catchments, except catchments of the fifth order. This implies that all order catchments follow Horton's second law, while the observed deviation in catchments of the fifth order indicates a variation in relief (Argyriou et al., 2017). The stream lengths present negative deviations from the ideal values for the second (−31.50%), third (−22.22%), and fifth (−66.24%) orders. This indicates that these streams are short because they are still in a youthful phase of development, which suggests that these streams cannot drain their area satisfactorily. The streams of smaller lengths are found in regions with larger slopes and smoother topography (Waikar and Nilawar, 2014). In contrast, the mean estimate of fourth-order stream lengths presents positive deviations (52.67%) from ideal values, which indicates more extensive and well-developed stream lengths (Table 2, Fig. 4b).

3.4. Drainage density (D)

The drainage density of third-order catchments ranges from 1.50 to 3.10 km^{-1} with a mean value of 2.26 km^{-1}

Table 2
Horton's first and second laws for the hydrographic complex of Samos Island.

Stream order (u)	Streams number (*Nu*)	Bifurcation ratio (***Rb***)	Mean bifurcation ratio ($\overline{\boldsymbol{Rb}}$)	Ideal streams number	Deviation (%)	Streams length (*Lu*)	Mean streams length ($\overline{\boldsymbol{Lu}}$)	Length ratio (***RL***)	Mean length ratio ($\overline{\boldsymbol{RL}}$)	Ideal mean streams length	Deviation (%)
1	869		4.60	448	93.97	486.6	0.56		2.27	0.56	0.0
2	234	3.71		97	141.23	203.4	0.87	1.55		1.27	−31.50
3	47	4.98		21	123.80	105.1	2.24	2.57		2.88	−22.22
4	10	4.70		5	100	29.02	10	4.46		6.55	52.67
5	2	5		1	100	10.03	5.02	0.50		14.87	−66.24
	$\Sigma Nu = 1162$					**$\Sigma Lu = 834.15$ (km)**					

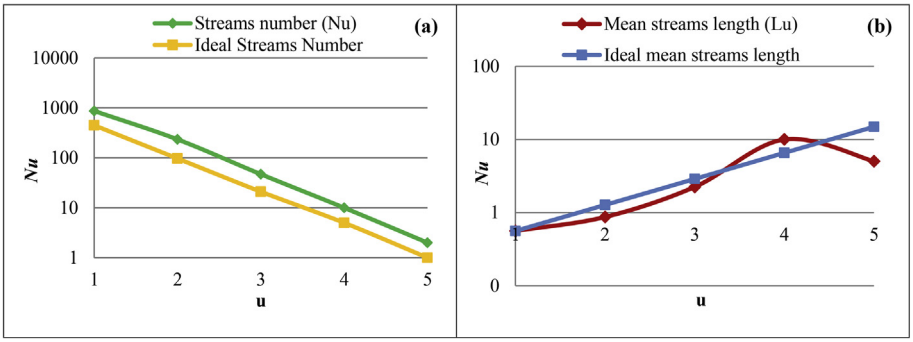

Fig. 4. **(a)** Deviation from ideal streams number per order according to Horton's first law. **(b)** Deviation from the ideal mean streams length per order according to Horton's second law.

(Table 3). The *D* values for the fourth- and fifth-order catchments range from 1.61 to 2.63 km^{-1} (mean value 2.04 km^{-1}) and 2.06 to 2.30 km^{-1} (mean value 2.18 km^{-1}) (Table 3). The *D* values in the third-, fourth- and fifth-order catchments show large variations, corresponding to various geographical developments and climatic regions. Low *D* values indicate inefficient drainage in the hydrographic network. *D* can influence the shape of a river's hydrologic response during a rainstorm. Rivers that have a low drainage density will not be prone to flash floods (Jackson, 2012). The *D* values are presented in Fig. S5a.

3.5. Channel frequency (F)

The third-order catchments have a channel frequency from 1.21 to 10.56 km^{-2}, with a mean value of 3.88 km^{-2}. For the fourth- and fifth-order catchments, *F* values are 1.61–5.46 km^{-2} (mean value 3.10 km^{-2}) and from 2.48 to 3.19 km^{-2} (mean value 2.84 km^{-2}), respectively (Table 3, Fig. S5b). The high values of channel frequency (>5) are associated with impermeable subsurface material, high relief, and low infiltration capacity, while low values (<5) imply high permeability geology, low relief and high infiltration capacity (Argyriou et al., 2017).

3.6. Relief ratio (Rh)

The relief ratio (*Rh*) is a dimensionless number that captures the overall slope of a drainage basin (Schumm, 1956) and indicates erosion, flooding seriousness, and sediment delivery processes (Strahler, 1957) that occur in the branches of the catchment. *Rh* is considered one of the essential morphometric parameters. In the third-order catchments, the relief ratio values range from 0.06 to 0.80, with a mean range of 0.20 (Table 3, Fig. S5c). In the fourth-order catchments, the *Rh* values range from 0.08 to 0.30, with a mean value of 0.14, and in the fifth-order catchments, *Rh* is 0.09 for both catchments of this order (with a mean value of 0.09) (Table 3, Fig. S5c). These values suggest that erosion rates in the third-order catchments are greater than those in the fourth-order catchments and even greater than those in the fifth-order catchments. Vavliakis (2002) confirmed these findings through the installation of a network of test surfaces to determine erosion processes in Samos Island. He found that in the higher-order catchments the erosion processes were smoother than the lower-order catchments. In the catchments of the Skiathos Island—western Aegean area, Dalaris et al. (2013) found that the erosion was greater in the lower-order catchments than in the higher ones. The large area in higher-order catchments helps to develop a better stream network than the small area in lower order catchments, and this leads to effective drainage, which makes erosion phenomena smoother (Dash et al., 2014). Other studies from the Balkan Peninsula (Gavrilovic et al., 2008) and Iran (Solaimani et al., 2009) display comparative outcomes.

3.7. Hypsometrical integral (H_I)

The hypsometrical integral (H_I) is a function of the topographic dissection (Pavano et al., 2018) and can be used as a measure of landscape maturity (Strahler, 1952). The H_I values are computed using the formula displayed in Table 1 (Keller and Pinter, 2002). According to Strahler (1952, 1957, 1964), the transition from the youth stage to the maturity stage corresponds approximately to a 60% H_I value, and the transition from the maturity stage to the ageing stage corresponds to a 35% H_I value. We observe that the H_I values of the third-order catchments extend from 19.42 to 63.34%, with a mean estimate of 45.54% (Table 3, Fig. S5d). All the third-order catchments are in the maturity stage, with the exception of two and three catchments, which are in the

Table 3
Morphometric parameters of Samos Island.

Order catchment	Drainage density (*D*) (km^{-1})			Channel frequency (*F*) (km^{-2})			Relief ratio (*Rh*) (%)			Hypsometric integral (H_I) (%)		
	min	max	mean	min	max	mean	min	max	mean	min	max	mean
Third	1.50	3.10	2.26	1.21	10.56	3.88	0.06	0.80	0.20	19.42	63.34	45.54
Fourth	1.61	2.63	2.04	1.61	5.46	3.10	0.08	0.30	0.14	23.00	55.79	37.27
Fifth	2.06	2.30	2.18	2.48	3.19	2.84	0.09	0.09	0.09	33.85	47.16	40.51

youth and ageing stages, respectively (Fig. S5d). The fourth-order catchments in the central part of the island and the catchment in the eastern part of the Island, near the limestone formations, are in the maturity stage. The other fourth-order catchments are in the ageing stage. Three of the catchments are located in the two Neogenic deposits of Samos, and one catchment is located in the western–southern part of Samos (Fig. S5d). Their values range from 23.00 to 55.79%, with an average value of 37.27% (Table 3). The northern fifth-order catchment is in the maturity stage, with a H_I value of 47.16%, and the southern fifth-order catchment is in the ageing stage, with a H_I value of 33.85% (Table 3). The different maturities between catchments of the same order are connected to their size (Fig. S5d), as smaller drainage basins tend to have larger H_I values (Chen et al., 2003; Dash et al., 2014).

3.8. Relief slopes classification

The relief slopes are essential components of the complex landscape that form a drainage basin (Chorley, 1957), and for this reason, their study is of great importance. The relief slopes were grouped based on the six major categories outlined by the classification of the International Geographical Union (IGU) (Demek et al., 1972) (Table 4). The most prominent extent of the Samos zone (35.14%) is described by slopes extending from 15° to 35°.

These values represent a rough to exceptionally rough relief, which is characterized by extreme events of rill erosion and denudation. These values are found in regions all over Samos Island (Fig. S6). The second highest extent of the Samos region (24.11%) is portrayed by slopes extending from 35° to 55°, and the third highest extent (15.84%) is indicated by slopes that are higher than 55°. These values are primarily observed in the areas of Ampelos in the northern and central parts of the island, as well as in Kerketeas in the western part (Fig. S6). These values represent a very rough to vertical relief, and they have endured serious denudation and demonstrate the extremely rough topography of Samos Island. The lower slope values, from 0° to 2° (5.6%) and 2°–5° (6.55%), represent the flat up to slightly inclined relief and correspond to flood fields, levelling surfaces, and valley foothills. They are located in the northern and southeastern parts of the island (Fig. S6).

3.9. Rose diagrams – plots (Rf)

Concerning hydrography, rose diagrams indicate that most of the first- and second-order streams are in the NE–SW direction (Figs. S8a–b). The third-order branches are in the north–south direction, while the branches of high orders (fourth and fifth) are in the NW–SE direction (Figs. S8c–e). The rose diagrams reveal two hydrographic network systems: an older hydrographic network system with a main NW–SE direction, which includes the higher branches, and a recent hydrographic network system with a main NE–SW direction, which includes the new, smaller order branches. Concerning tectonic faults (Fig. S7), the rose diagrams were grouped based on the five previously mentioned geomorphological zones of Samos. It is presumed that in both the eastern and western regions of Samos, the major trends are NNW–SSE (Figs. S9a and e). The major trends for both Neogenic deposits are west–east, and the minor trends are NW–SE for the eastern region and NWW–SEE for the western region (Figs. S9b and d). In central Samos, there is a primary west–east trend and an extremely slight NWW–SEE trend (Fig. S9c). The impact of tectonic faults on the hydrographic network was determined by the correlation between the trends of the tectonic faults (Fig. S9ae) indicated by the rose diagrams and the branches of the drainage networks (Figs. S8a–e). The orientation of the major tectonic faults in the study area, as expressed above, is NNW–SSE. The direction of the first- and second-order streams is mainly NE–SW oriented, and the third-order streams mainly flowed in the north–south direction. These directions do not match the faults' orientations. The dominant orientations of the fourth- and fifth-order streams are NW–SE and do not match the trend of the faults. Taking everything into account, the tectonic regime has a non-significant impact on the development of the stream network pattern of Samos Island.

Table 4
Relief slope classification of Samos Island catchment according to IGU (Demek et al., 1972).

Slope angle	Surface in km^2	Percentage of total surface (%)
0–2°	26.84	5.6
2–5°	31.36	6.55
5–15°	60.95	12.73
15–35°	168.17	35.14
35–55°	115.37	24.11
>55°	75.80	15.84

4. Conclusions

In this study, we analysed the drainage system of Samos Island to determine erosion capacity, susceptibility to floods, and the interplay between the tectonics and the drainage basin morphology. The results indicate that Samos is a fifth-order basin. The hydrographic network has short stream lengths for third- and fifth-order catchments, which indicates a non-satisfactory drainage capacity and a vulnerability to erosion phenomena. The finding is enhanced by the prevalence of slopes ranging from 15° to 35°, which suggests intense erosion events and denudation. The catchments developed at different geographical formations and microclimatic regions exhibit a variable drainage density, while the impermeable subsurface material and high-relief and low-infiltration capacity produce high channel frequency values in some third- and fourth-order catchments. The relief ratio shows that the erosion processes occurring in the third-order catchments are more serious than those of higher (fourth and fifth) orders. This is associated with the fact that, in lower-order catchments, the hydrographic network is younger and unable to satisfactorily drain the area, which leads to erosion phenomena, unlike in higher order catchments, where the large area favours the development of the hydrographic network, thus making erosion events smoother. As indicated by hypsometrical integral analysis, most of the third-order catchments are in the youth and maturity stages. The

fourth- and fifth-order catchments are in the maturity and ageing stages. The different maturities between catchments of the same order appear to be dependent on their size. Two different hydrographic network systems appeared in the study area: an older hydrographic network system with a main NW–SE direction, which includes the fourth- and fifth-order branches, and a younger hydrographic network with a main direction of NE–SW, which includes new, smaller-order branches. The major tectonic structures (nappes contacts) are NNW–SSE. The superposition of rose diagrams of the hydrographic network and tectonic faults of Samos Island indicate that the flow directions of the streams do not match the faults' orientations, which indicates that the tectonic faults do not affect the development of the drainage system.

Appendix A. Supplementary data

Supplementary data to this article can be found online at https://doi.org/10.1016/j.crte.2019.03.001.

References

Angilliri, Y.E., 2008. Morphometric analysis of Colanguil river basin and flash flood hazard, San Juan, Argentina. Environ. Geol. 55 (1), 107–111.

Apollov, B.A., 1963. A Study of Rivers. Moscow University, Moscow.

Argyriou, A.V., Teeuw, R.M., Soupios, P., Apostolos Sarris, A., 2017. Neotectonic control on drainage systems: GIS-based geomorphometric and morphotectonic assessment for Crete, Greece. J. Struct. Geol. 104, 93-11.

Arnous, M.O., Omar, A.,E., 2018. Hydrometeorological hazards assessment of some basins in southwestern Sinai area, Egypt. J. Cost. Conserv. 22, 721–743.

Bahrami, S., 2013. Analyzing the drainage system anomaly of Zagros basins: implications for active tectonics. Tectonophysics 608, 914–928.

Bhagwat, T.N., Shetty, A., Hegde, V.S., 2011. Spatial variation in drainage characteristics and geomorphic instantaneous unit hydrograph (GIUH); implications for watershed management–A case study of the Varada River basin, Northern Karnataka. Catena 87 (1), 52–59.

Chen, Y., Sung, Q., Cheng, K., 2003. Along-strike variations of morphotectonic features in the western foothills of Taiwan: tectonic implications based on stream-gradient and hypsometric analysis. Geomorphology 56 (1), 109–137.

Chorley, R.J., 1957. Illustrating the laws of morphometry. Geol. Mag. 94, 140–149.

Cooper, A.H., Farrant, A.R., Price, S.J., 2011. The use of karst geomorphology for planning, hazard avoidance and development in Great Britain. Geomorphology 134 (1–2), 118–131.

Dalaris, M., Psilovikos, Ar, Sapountzis, M., Mourtzios, P., 2013. Water erosion assessment in Skiathos island using the Gavrilović method. Fresenius Environ. Bull. 22 (10), 2943–2952.

Dash, P., Aggarwal, S.P., Verma, N., Ghosh, S., 2014. Investigation of scale dependence and geomorphic stages of evolution through hypsometric analysis: a case study of Sirsa basin, western Himalaya, India. Geocarto Int. 29 (7), 758–777.

Demek, J., Embleton, C., Gellert, J.F., Verstappen, H.T., 1972. Manual of Detailed Geomorphological Mapping. In: International Geographical Union Commission on Geomorphological Survey and Mapping. Academia, Prague.

Dermitzakis, M., Papanikolaou, D., 1981. Paleogeography and geodynamics of the Aegean Region during the Neogene, Annales géologiques des pays helléniques. In: Proceedings of the VIIth International Congress on Mediterranean Neogene, Athens, 27 September–2 October 1979, pp. 245–288.

Gavrilovic, Z., Stwfanovic, M., Milovanovic, I., Cotric, J., Milojevic, M., 2008. Torrent classification- base of rational management of erosive regions. In: Proceedings of the XXIVth Conference of the Danubian Countries. Bled, Slovenia.

Hajam, R.A., Hamid, A., Bhat, S., 2013. Application of morphometric analysis for geohydrological studies using geo-spatial technology- A case study of Vishav drainage basin. Hydrol. Curr. Res. 4 (3).

HMGS (Hellenic Military Geographical Service), 1978. Topographical maps, sheets "Samos" & "Neon Karlovasion", scale 1:50 000.

Horton, R.E., 1932. Drainage basin characteristics. Trans. Am. Geophys. Union 13, 350–361.

Horton, R.E., 1940. An approach toward a physical interpretation of infiltration capacity. Soil Sci. Soc. Am. J. 5, 399–417.

Horton, R.E., 1945. Erosional development of streams and their drainage basins, hydrophysical approach to quantitative morphology. Geol. Soc. Am. Bull. 56, 275–370.

IGME (Institute of Geology and Mineral Exploration), 1985. Geological maps, sheets "Samos" & "Neon Karlovasion", scale 1:50 000.

Jackson, A., 2012. Discharge & Hydrographs. Geography AS Notes. https://geographyas.info/rivers/discharge-and-hydrographs/. (Accessed December 2011).

Jahan, C.S., Rahaman, M.F., Arefin, R., et al., 2018. Morphometric analysis and hydrological inference for water resource management in atraisib river basin, NW Bangladesh using remote sensing and GIS technique. J. Geol. Soc. India 91, 613.

Kantiranis, N., Stamatakis, M., Filippidis, A., Squires, C., 2004. The uptake ability of the clinoptilolitic tuffs of Samos Island, Greece. Bull. Geol. Soc. Greece XXXVI, 89–96.

Keller, E.A., Pinter, N., 2002. Active Tectonics: Earthquakes, Uplift, and Landscape, second ed. Prentice Hall, New York.

Kotinas, V., 2014. Study of Flood and Soil Erosion on the Island of Samos, Using Artificial Intelligence Methods and GIS. Master Dissertation. National and Kapodistrian University of Athens.

Kumar, D., Singh, D.S., Prajapati, S.K., et al., 2018. Morphometric parameters and neotectonics of Kalyani River Basin, Ganga Plain: a remote sensing and GIS approach. J. Geol. Soc. India 91, 679.

Kumar, R., Kumar, S., Lohani, A.K., Nema, R.K., Singh, R.D., 2000. Evaluation of geomorphological characteristics of a catchment using GIS. GIS India 9 (3), 13–17.

Mourtzios, P., Psilovikos, Ar, Astaras, T., 2009. Geomorphologic and hydrologic analysis of Torrent Imvrassos in Samos Island, using GIS. Assessment of flooding hazard. In: Proceedings of the 2nd International Conference on Environmental Management, Engineering, Planning and Economics (CEMEPE), Mykonos, Greece, vol. III, pp. 1729–1734.

Ngapna, M.N., Owona, S., Owono, F.M., et al., 2018. Tectonics, lithology and climate controls of morphometric parameters of the Edea–Eseka region (SW Cameroon, Central Africa): implications on equatorial rivers and landforms. J. Afr. Earth Sci. 138, 219–232.

Ntokos, D., 2017. Formulation of the conceptual model for the tectonic geomorphological evolution of an area: five main rivers of Greece as a case study. Catena 167, 60–77.

Pareta, K., Pareta, U., 2011. Quantitative morphometric analysis of a watershed of Yamuna basin, India using ASTER (DEM) data and GIS. Int. J. Geomatics Geosci. 2 (1), 248–269.

Pavano, F., Catalano, S., Romagnoli, G., Tortorici, G., 2018. Hypsometry and relief analysis of the southern termination of the Calabrian arc, NE-Sicily (southern Italy). Geomorphology 304, 74–88.

Peel, M.C., Finlayson, B.L., McMahon, T.A., 2007. Updated world map of the Köppen–Geiger climate classification. Hydrol. Environ. Syst. Sci. 11, 1633–1644.

Perucca, L.P., Angilieri, Y.E., 2010. Morphometric characterization of delMolle Basin applied to the evolution of flash floods hazards, Iglesia Department, San Jaun, Argentina. Quat. Int. 233 (1), 81–86.

Psilovikos, Ar, Margoni, S., Vavliakis, E., Psilovikos, Ant, 2004. Monitoring and simulation of the geographic distribution of the rainfall of 28 – 29/11/2001 in Samos island. Contribution in the integrated management of water resources. In: Proceedings of the 7th PanHellenic Geographic Conference, Mitilini, Greece, Vol. I, pp. 450–457.

Psilovikos, Ar, Vavliakis, E., Margoni, S., Koutalou, V., 2003. Determination of the runoff coefficient in the hydrological basins of the main torrents in Samos island after the fire of 2000 using orthophotomaps and G.I.S. In: International Symposium GIS and Remote Sensing: Environmental Applications, Volos, Greece, pp. 307–314.

Ribolini, A., Spagnolo, M., 2008. Drainage network geometry versus tectonics in the Argentera massif (French–Italian alps). Geomorphology 93, 3–4.

Schumm, S.A., 1956. Evolution of drainage complexes and slopes in badlands at Perth Amboy, New Jersey. Bull. Geol. Soc. Am. 67, 597–646.

Shreve, L., 1966. Statistical law of stream numbers. J. Geol. 74, 17–37.

Solaimani, K., Modallaldoust, S., Lotfi, S., 2009. Soil erosion prediction based on land use changes (A case in Neka watershed). Am. J. Agric. Biol. Sci. 4 (2), 97–104.

Stamatakis, M., 1989a. Authigenic silicates and silica polymorphs in the Miocene saline-alkaline deposits of the Karlovassi basin, Samos Island, Greece. Econ. Geol. 84, 788–798.
Stamatakis, M., 1989b. A boron-bearing potassium feldspar in volcanic ash and the tuffaceous rocks from Miocene lake deposits, Samos Island, Greece. Am. Mineral. 74, 230–235.
Strahler, A.N., 1952. Hypsometric (arc – altitude) analysis of erosional topography. Bull. Geol. Soc. Am. 63, 1117–1142.
Strahler, A.N., 1957. Quantitative analysis of watershed geomorphology. Trans. Am. Geophys. Union 38, 913–920.
Strahler, A.N., 1964. Quantitative geomorphology of drainage basins and channel networks. In: Chow, V.T. (Ed.), Handbook of Applied Hydrology. McGraw-Hill, New York, pp. 439–476.
Vassilopoulos, A., Evelpidou, N., Tziritis, E., Boglis, A., 2008. Wetlands the Pattern of Samos Island. Faculty of Geology and Geoenvironment, University of Athens.
Vavliakis, E., 2002. Monitoring the Changes on the Burned Areas of Samos Island and the Effects in Land Erosion, Flooding Episodes and Water Resources. Research committee of Aristotle University of Thessaloniki, Greece.
Verstappen, H.Th., 1983. The Applied Geomorphology. Int. Ins. Aer. Surv. Earth Sci. (ITC). Enschede, The Netherlands.
Waikar, M.L., Nilawar, A.P., 2014. Morphometric analysis of a drainage basin using geographical information complex: a case study. Int. J. Multidisciplinary and Current Research 2, 179–184. http://www.hnms.gr/emy/el/.